Pergamon

1359-6454(95)00425-4

Acta mater. Vol. 44, No. 8, pp. 3429–3438, 1996
Published by Elsevier Science Ltd
Printed in Great Britain
1359-6454/96 $15.00 + 0.00

NONEQUILIBRIUM THERMODYNAMICS OF FERROELECTRIC DOMAIN EVOLUTION

R. E. LOGE and Z. SUO

Mechanical and Environmental Engineering Department, Materials Department, University of California, Santa Barbara, CA 93106, U.S.A.

(Received 30 May 1995)

Abstract—A ferroelectric crystal tends to form domains. Internal and external fields can cause domain walls to move, resulting in macroscopic phenomena such as aging, creep and fatigue. Domain evolution is a nonequilibrium thermodynamic process. The domain pattern, the state of the crystal, can be described with a set of generalized coordinates. The free energy of the crystal is a function of the generalized coordinates, to be pictured as a surface in the thermodynamic space, the free energy erecting and the generalized coordinates spanning. A point on this surface represents a (nonequilibrium) state of the crystal, the slopes of the tangent plane contacting the surface at the point are the generalized forces, and a curve on the surface is an evolution path. Thermodynamics requires that the path descend on the surface, but by itself does not determine the path. To complete this global picture of structural evolution, we formulate a variational principle that includes kinetics. The functional to be minimized consists of the free energy rate and a dissipation potential involving the domain wall mobility. The variational principle equips a viscosity matrix to every point on the thermodynamic surface. The approach results in a set of ordinary differential equations that govern the evolution of the generalized coordinates. We outline the operational aspects of this approach, make contact with the finite element method, and illustrate the approach by examples of one or two degrees of freedom.

1. INTRODUCTION

Barium titanate ($BaTiO_3$) undergoes a phase transition at a temperature of about 130°C. Figure 1 shows the unit cells of the two phases, paraelectric and ferroelectric. Above 130°C, the crystal is cubic, and the ions lie symmetrically in the unit cell. Between 0 and 130°C, the crystal is tetragonal, and the ions lie asymmetrically in the unit cell. A tetragonal unit cell may have polar direction of any of the six variants. A load can rotate the polar axis from one direction to another. Figure 2 illustrates several possibilities. An electric field may rotate the polar direction by either 180 or 90°, but a stress may only rotate it by 90°. A 180° polar rotation does not result in any strain; a 90° polar rotation results in a large strain. We will use barium titanate to illustrate the various points in this paper. Table 1 lists the representative data to be used in numerical examples.

The crystal changes its state progressively by domain wall movements. The loads needed to move the domain walls are much lower than the loads theoretically predicted to uniformly switch the crystal [1]. In fact, the latter has never been observed. The higher the loads and the temperature, the faster the wall motion. In $BaTiO_3$, the domain walls are observed to move at a wide range of velocities (10^{-9}–10^{-1} m/s) [2].

Domain wall movements underlie all phenomena of polarization and deformation. They have profound effects on the devices made of ferroelectrics, usually in polycrystalline (i.e. ceramic) forms. Upon cooling through the paraelectric-to-ferroelectric transition temperature, a ceramic forms domains that result in no net polarization. An electric field may pole the ceramic. In storage under the internal field, the ceramic may age and its state changing gradually [3]. Subject to a small fixed load, the ceramic may creep, its polarization or strain increasing slowly [3, 4]. Under a cyclic voltage, the ceramic may fatigue and its remanent polarization decreasing with cycles [5]. Ceramics in general contain impurities that make them "hard" [3].

Domain evolution is a nonequilibrium thermodynamic process. We will adopt an approach similar to an approach to modeling grain growth. In grain growth, the free energy is the surface tension summed over all the grain boundaries. The reduction in the free energy, associated with a unit area of a grain boundary moving a unit distance, defines a thermodynamic force, the driving pressure. This pressure moves the grain boundary at a velocity according to an empirical law [6, 7]. The free energy of a ferroelectric crystal must include, in addition to the surface tension of the domain walls, the energy stored inside the domains and the work done by the external loads. An expression of the pressure has been derived recently [8, 9]. We call this the local approach.

In this paper, we describe a global approach on the basis of a variational principle. In Section 2 we apply

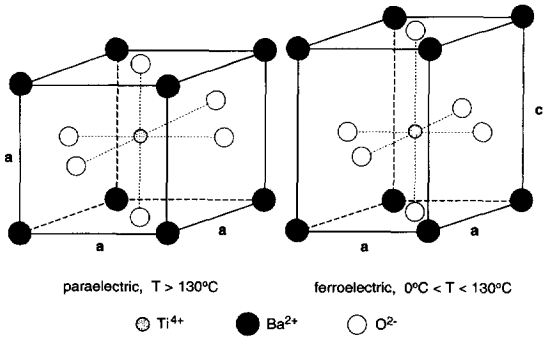

Fig. 1. The crystal structures of barium titanate ($BaTiO_3$). The high temperature phase is nonpolar. The low temperature phase is polar and the Ti ion is off the cell center.

the nonequilibrium thermodynamics to domain evolution. The local approach is summarized and the variational principle introduced. In Section 3, we idealize the energetic and kinetic descriptions, apply the Rayleigh–Ritz method on the basis of the variational principle, and discuss its implementation within the finite element method. The dynamic system has both a physical length scale and a time scale. The remaining sections of the paper illustrate this global approach with examples of one or two degrees of freedom. Section 4 shows how the basic parameters in the model, the domain wall mobility and energy, may be obtained from experiments. Section 5 approximates a domain nucleus as a sequence of evolving ellipses.

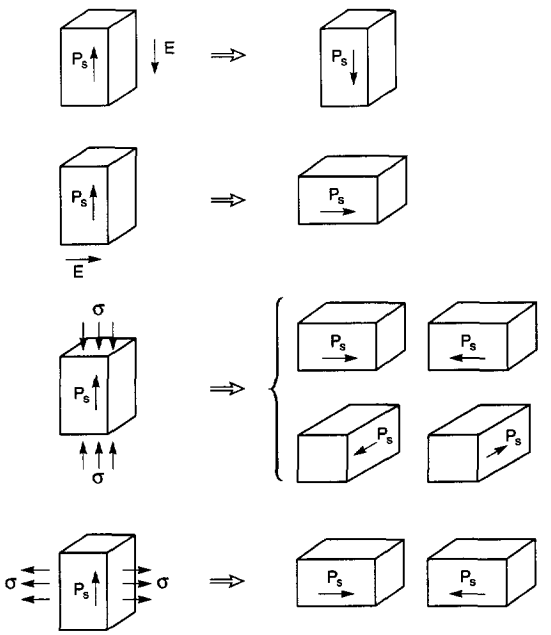

Fig. 2. In the ferroelectric phase, barium titanate has six variants of the polar direction. P_s is the spontaneous polarization. An electric field or a stress can switch the crystal from one variant to another.

Table 1. Data used in numerical examples

Spontaneous polarization	$P_s = 0.26$ C/m^2
Permittivity	$\varepsilon = 10^{-8}$ F/m
180° domain wall energy	$\Gamma = 0.01$ J/m^2
90° domain wall energy	$\Gamma = 0.002$ J/m^2
Spontaneous strain	$\gamma_s = 0.01$
Shear modulus	$\mu = 3 \times 10^{10}$ N/m^2
Poisson's ratio	$\nu = 1/3$
180° domain wall mobility	$M = 4.8 \times 10^{-4}$ m^3/s N

2. DOMAIN EVOLUTION IS A NONEQUILIBRIUM THERMODYNAMIC PROCESS

We now apply the nonequilibrium thermodynamics [10] to a polydomain ferroelectric crystal. For a large range of applications, domain walls move slow enough for the crystal to maintain thermal, mechanical and electrical equilibrium. Domain wall motion is taken to be the nonequilibrium, rate-limiting process; we thus avoid treating impurity diffusion and dislocation motion. The crystal has a uniform temperature, T; the stress and the electric fields obey the following static field equations.

2.1. *Static field equations*

Subject the crystal to a field of displacement **u** and electric potential ϕ, and their gradients give the strain tensor γ and the electrical field vector **E**:

$$\gamma_{ij} = \tfrac{1}{2}(u_{i,j} + u_{j,i}), \quad E_i = -\phi_{,i}. \tag{2.1}$$

The standard index notation is adopted. Let **t** be the force and ω the charge, per unit area, externally supplied on an interface between two media. The body force and the space charge inside the domains are taken to be negligible. In a dielectric both stress tensor $\boldsymbol{\sigma}$ and electric displacement vector **D** are divergence free

$$\sigma_{ij,i} = 0, \quad D_{i,i} = 0. \tag{2.2}$$

Across an interface between two media labeled as + and −, they jump by

$$n_i[\sigma_{ij}^- - \sigma_{ij}^+] = t_j, \; n_i[D_i^- - D_i^+] = -\omega. \tag{2.3}$$

The unit vector normal to the interface, **n**, points to medium +. If no external force and charge lie on a domain wall, $t_j = 0$ and $\omega = 0$, the traction $n_i\sigma_{ij}$ and the normal component of the electric displacement n_iD_i are continuous across the domain wall.

2.2. *Energetics and kinetics*

Prescribe a distribution of traction **t** and electric potential ϕ on the external surface of the crystal. On the part of the surface where the electric potential is not prescribed, e.g. the interface between the crystal and the air, we assume that negligible electric field lines escape from the crystal. This is a good approximation because a typical ferroelectric has an enormous permittivity. Consequently, the prescribed

electric potential does work on the crystal, not on the air.

We will make the standard local equilibrium assumption. That is, a free energy function exists for every small element of the crystal, even though the crystal as a whole is not in equilibrium. The free energy of the entire crystal is summed over the elements. The crystal stores energy in the domain walls and in the domains. Denote the surface energy per unit area of a domain wall by Γ. At a fixed temperature, the Helmholtz free energy per unit volume of a domain, ψ, is a function of the electric displacement and the strain, varying according to

$$d\psi = E_i\, dD_i + \sigma_{ij}\, d\gamma_{ji}. \tag{2.4}$$

The differential coefficients are the stress and the electric field. The function $\psi(\mathbf{D}, \gamma)$ may be determined empirically [11,12].

A ferroelectric domain is a sharp transition within a few atomic layers. The electro-mechanical field is taken to be unaffected by the domain wall energy and the domain wall energy unaffected by the electro-mechanical field. The combination of the function $\psi(\mathbf{D}, \gamma)$ and the field equations in Section 2.1 defines an electro-mechanical boundary value problem.

Once the static field is solved at a given crystal state, the Gibbs free energy of the entire crystal is calculated from

$$G = \int \Gamma\, dA + \int \psi\, dV - \int \phi\omega\, dA - \int t_i u_i\, dA. \tag{2.5}$$

The first integral extends over the domain walls, the second over the domains, the third over the potential-prescribed surface, and the fourth over the traction-prescribed surface.

Imagine that domain walls undergo a small virtual motion. The amount of motion may differ from element to element on the walls. Let δr be a distribution of the virtual displacement normal to the domain walls, and δG the free energy change in the crystal associated with this virtual motion. The thermodynamic pressure, p, is the reduction in the free energy associated with a unit area of the domain wall advancing a unit distance. Thus,

$$\delta G + \int p\delta r\, dA = 0 \tag{2.6}$$

holds for any virtual motion, the integral being over all domain walls. This equation uniquely defines the pressure.

The pressure p drives an element of a domain wall to move at a velocity V, in the direction normal to the wall, according to a law [8, 9]

$$p = F(V). \tag{2.7}$$

The function F specifies the rate of atomic shuffling. It may vary from element to element because of heterogeneity or anisotropy. In practice, the kinetic law is determined experimentally by its macroscopic consequences.

This approach regards a domain wall as a continuum surface moving in space. It is generally believed, however, that domain walls move as step kink-like dislocations [13, 14]. The same ambiguity, to various degrees, exists in modeling grain growth and surface reaction in this way. The validity of this approach to ferroelectric domain evolution remains to be ascertained by comparing its predictions with experiments.

2.3. *Local approach*

Recall the Eshelby momentum tensor [15]

$$P_{ij} = \psi\delta_{ij} - \sigma_{ik}\gamma_{kj} - E_i D_j. \tag{2.8}$$

We add the electric term by analogy. Consider a wall between domain + and domain −, the unit normal vector $\mathbf{n}$ pointing toward domain +. Denote the sum of the principal curvatures of the domain wall by κ, being positive if the center of the curvature is in domain +. Assume that no external force or charge lie on the domain wall. When an element of the domain wall moves in the direction $\mathbf{n}$ by a distance δr, the free energy of the crystal changes by [8, 9, 15, 16]

$$\delta G = -\int [\Gamma\kappa + n_i(P_{ij}^{+} - P_{ij}^{-})n_j]\delta r\, dA. \tag{2.9}$$

We add the domain wall energy term, assuming a constant Γ; see Ref. [17] for anisotropic Γ.

A comparison of equations (2.9) and (2.6) gives

$$p = \Gamma\kappa + n_i(P_{ij}^{+} - P_{ij}^{-})n_j. \tag{2.10}$$

This formula relates the thermodynamic pressure to the local quantities. Special cases of equation (2.10) have appeared in many surface motion problems. The first term is the Laplace–Young formula for soap bubbles, applicable to grain growth [6, 7] and solid surface evolution [18]. If medium − is taken to be a traction-free but strained solid, and medium + the vacuum, equation (2.10) becomes $p = \Gamma\kappa - \psi$. Asaro and Tiller [19] obtained this formula in analyzing surface motion.

An approach to tracing the evolution of a domain pattern is as follows. For a given domain pattern, the static field is solved as a boundary value problem, the pressure computed from equation (2.10), and the velocity from equation (2.7). The velocity then updates the domain pattern for a small time step. This approach is called the local approach.

2.4. *Variational principle*

We now introduce a variational principle that will form the basis for a global approach. Define a dissipation potential

$$\mathscr{D}(V) = \int_0^V F(\zeta)\, d\zeta. \tag{2.11}$$

Here F is the mobility function in equation (2.7). Thermodynamics requires that $F(V)V \geqslant 0$ [8, 9]. In addition, we will restrict F to be a monotonically increasing function so that $F' > 0$. The consequence of this latter restriction will become evident.

Let U be a distribution of virtual velocity in the direction normal to the domain walls. (A virtual velocity may not satisfy the kinetic relation, but the actual velocity does.) Associated with this virtual motion, the free energy changes at rate $\dot{G}(U)$. The superimposed dot means the time rate. We now state the variational principle. Of all virtual velocity distributions U, the actual velocity distribution V minimizes the functional

$$\Pi(U) = \dot{G}(U) + \int \mathscr{D}(U)\, \mathrm{d}A. \qquad (2.12)$$

Note that Π is a functional of velocity. The state of the crystal—the domain pattern and the static field—is fixed when calculating Π at each time step.

To prove the principle, let V be the actual velocity, and U be a virtual velocity, so that $U + V$ is also a virtual velocity. Since the free energy is independent of the velocity, the free energy rate is linear in the velocity. Thus,

$$\dot{G}(V + U) - \dot{G}(V) = \dot{G}(U).$$

Take the Taylor expansion of the dissipation potential

$$\mathscr{D}(V + U) - \mathscr{D}(V) = F(V)U + \tfrac{1}{2}F'(\xi)U^2,$$

where ξ lies between V and $V + U$. A combination of the above gives the variation in Π

$$\Pi(V + U) - \Pi(V) = \dot{G}(U) + \int F(V)U\, \mathrm{dA} + \int \tfrac{1}{2}F'(\xi)U^2\, \mathrm{d}A.$$

The first two terms cancel each other because of equations (2.6) and (2.7). The remaining term is non-negative because $F' > 0$. Consequently, $\Pi(V + U) - \Pi(V) \geqslant 0$ for any virtual velocity. Thus, the proof. The above also demonstrates that the actual velocity distribution is uniquely determined by the current state of the crystal. Evidently, the uniqueness results from a monotonic kinetic function.

3. IDEALIZATIONS AND THE RAYLEIGH–RITZ METHOD

3.1. Deep energy basins

Far below the paraelectric-to-ferroelectric transition temperature, the Helmholtz free energy is non-convex and has deep basins [12]. Figure 3(a) illustrates the one-dimensional situation where ψ is a function of the electric displacement D, having two basins at P_s and $-P_s$, corresponding to spontaneous polar states. Due to crystal symmetry, the spontaneous states have the same free energy, ψ_0. Figure 3(b) shows the D–E curve derived from the free energy. The peak, E_c, is the field needed to switch polarization uniformly over the entire crystal, which is much larger than the field needed to cause domain wall motion. Consequently, we will use the linear D–E relation near the spontaneous polar states.

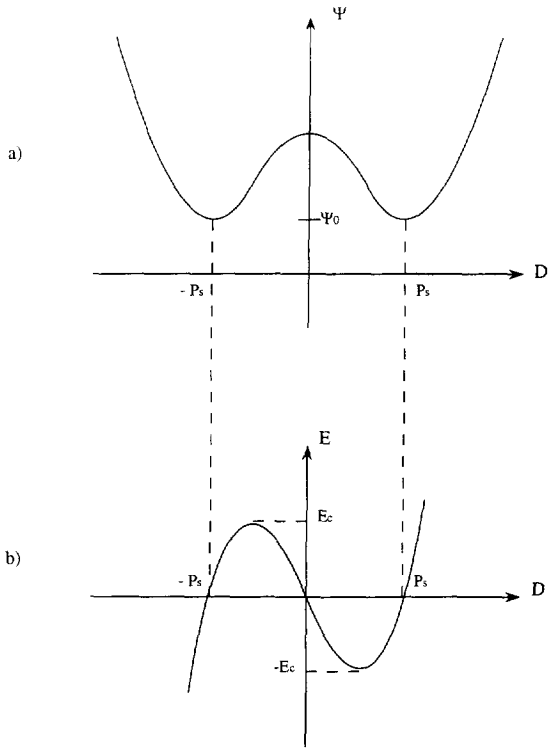

Fig. 3. (a) The Helmholtz free energy as a function of the electric displacement. The free energy has deep basins when the crystal is in the ferroelectric phase. (b) The theoretical electric field vs electric displacement curve. Only the linear part near the spontaneous state will be realized in a crystal.

In general, let $\gamma = \gamma^{(s)}$ and $\mathbf{D} = \mathbf{P}^{(s)}$ be a spontaneous polar state. Approximate the free energy around this state by the leading terms in the Taylor expansion, retaining up to the quadratic terms. Thus,

$$\psi^{(s)} = \psi_0 + \tfrac{1}{2}C^{(s)}_{ijkl}(\gamma_{ij} - \gamma^{(s)}_{ij})(\gamma_{kl} - \gamma^{(s)}_{kl}) + \tfrac{1}{2}\beta^{(s)}_{ik}(D_i - P^{(s)}_i)(D_k - P^{(s)}_k) + h^{(s)}_{ikl}(D_i - P^{(s)}_i)(\gamma_{kl} - \gamma^{(s)}_{kl}). \qquad (3.1)$$

Taking the partial differentiation according to equation (2.4), one obtains the linear relations

$$\sigma_{ij} = C^{(s)}_{ijkl}(\gamma_{kl} - \gamma^{(s)}_{kl}) + h^{(s)}_{kij}(D_k - P^{(s)}_k), \qquad (3.2)$$

$$E_i = \beta^{(s)}_{ik}(D_k - P^{(s)}_k) + h^{(s)}_{ikl}(\gamma_{kl} - \gamma^{(s)}_{kl}). \qquad (3.3)$$

The coefficients C, β and h characterize the elastic, dielectric and piezoelectric responses near the spontaneous state. Their values are available for barium titanate [3]. These linear relations are taken to be valid inside each domain. Together with the field equations in Section 2.1, they define a linear, coupled, electro-mechanical boundary value problem at a given crystal state.

3.2. Ideal kinetic laws

Under the creep or the aging conditions, the thermodynamic pressure is expected to be small, $p\Omega \ll kT$, where Ω is the volume of the unit cell, k

Boltzmann's constant, and T the absolute temperature. It may be justifiable to use a linear relation

$$V = Mp. \tag{3.4}$$

The mobility of M is independent of p, but depends on the temperature and the crystalline direction. Thermodynamics requires that $M > 0$. This simple law has been used in many surface motion problems, such as grain growth and surface reaction. We will use this law in all subsequent sections.

For a second kind of behavior, domain walls may move only when the driving pressure exceeds some critical point. The simplest law that captures this behavior is

$$V = \begin{cases} -\infty, p < -p_c \\ 0, |p| < p_c \\ +\infty, p > p_c. \end{cases} \tag{3.5}$$

This law will give time-independent macroscopic response.

A third kind of behavior involves a domain wall surrounded by an impurity atmosphere. A non-monotonic kinetic law may arise. Think of $p = F(V)$ as a law prescribing a resistance p when a domain wall moves at velocity V. At a low velocity, the impurity atmosphere migrates with the domain wall, and the resistance increases as the velocity increases. At some high velocity, the domain wall breaks away from its impurity atmosphere, and the resistance drops. Other kinetic laws for domain wall migration have been proposed in the literature [10].

3.3. *Rayleigh–Ritz method*

In the following illustrations, we will use the linear kinetic law, equation (3.4). The functional (2.12) becomes

$$\Pi(U) = \dot{G}(U) + \int \frac{U^2}{2M}\, dA. \tag{3.6}$$

Of all virtual velocities, the actual velocity minimizes Π.

Describe a domain pattern as a system of n degrees of freedom, writing $q_1, \ldots q_n$ for the generalized coordinates, and $\dot{q}_1, \ldots \dot{q}_n$ for the generalized velocities. The free energy is a function of the coordinates, but is independent of the velocities. The function $G(q_1, q_2, q_3, \ldots)$ is a surface in the space spanned by $G, q_1, \ldots q_n$. The state of the crystal is a point on the surface, and an evolution path is a curve on the surface. The generalized forces, $f_1, \ldots f_n$, are the differential coefficients of the free energy namely

$$dG = -f_1\, dq_1 - f_2\, dq_2 + \text{etc.} \tag{3.7}$$

At a given state of the crystal, i.e. a point on the thermodynamic surface, the forces are the slopes of the tangent plane contacting the surface at the point.

If the free energy function is known analytically, the forces can be computed by taking partial differentiation, $f_i = -\partial G/\partial q_i$. Examples in the following sections all belong to this category. In general, however, the free energy function is available only numerically at a crystal state. For example, if the domain pattern is modeled by finite elements, the positions of the nodes on the domain walls are the generalized coordinates. At each time step, the finite element analysis solves the static boundary value problem. Socrate and Parks [16] have recently described a procedure to compute the generalized forces within the framework of the finite element method.

Thermodynamics requires that the path descend on the free energy surface, but does not uniquely determine the direction of the path. We now show that the variational principle endows another property—a viscosity matrix—to every point on the thermodynamic surface. The combination of the forces and the viscosities uniquely determines the evolution direction and rate.

The virtual velocity of an element on the domain walls, U, is linear in the generalized velocities. Write

$$U = \sum_i N_i \dot{q}_i, \tag{3.8}$$

where N_i are the shape functions. Consequently, the dissipation term in the variational principle of equation (3.6) is quadratic in the generalized velocities

$$\frac{1}{2}\int \frac{U^2}{M}\, dA = \frac{1}{2}\sum_{i,j} H_{ij}\dot{q}_i\dot{q}_j, \tag{3.9}$$

with

$$H_{ij} = \int (N_i N_j/M)\, dA. \tag{3.10}$$

They form a symmetric, positive-definite matrix, which we call the viscosity matrix.

Now Π is a function of the generalized velocities,

$$\Pi(\dot{q}_1, \ldots, \dot{q}_n) = -\sum_i f_i\dot{q}_i + \frac{1}{2}\sum_{i,j} H_{ij}\dot{q}_i\dot{q}_j. \tag{3.11}$$

It minimizes when $\partial\Pi/\partial\dot{q}_k = 0$, leading to

$$\sum_i H_{ij}\dot{q}_i = f_i. \tag{3.12}$$

The significance of H as a viscosity matrix now becomes evident. This is a set of linear algebraic equations for the generalized velocities. Once solved, they update the generalized displacements for a small time step. The process is repeated for many steps to evolve the domain pattern.

3.4. *Length scale and time scale*

Load a crystal by electric field E_∞ and stress σ_∞. Let ε be a permittivity in some crystalline orientation, h

a piezoelectric modulus, and μ a shear modulus. The free energy of the crystal takes the form

$$G = a\Gamma + \frac{b_1}{2\varepsilon} P_s^2 + b_2 h P_s \gamma_s + \frac{b_3 \mu}{2} \gamma_s^2 - c_1 E_\infty P_s - c_2 \sigma_\infty \gamma_s. \quad (3.13)$$

The coefficient a has the dimension of area, and b and c of volume, to be determined by solving the static boundary value problem at a given crystal state. They depend on dimensionless ratios of electro-mechanical moduli in equations (3.2) and (3.3). The static boundary value problem is linear, so that a, b and c do not depend on P_s, γ_s, E_∞ and σ_∞. The first term in equation (3.13) is the domain wall energy, the next three terms are due to the field induced by the misfit among the domains, and the last two terms are the external work done to switch domains.

The dynamic system has both a characteristic length scale and a characteristic time scale. The domain wall energy, Γ, results from atomic scale interactions of a few layers of atoms making up the wall. The dielectric energy, P_s^2/ε, results from the long range electric interaction. Their ratio sets a characteristic length

$$l_0 = \Gamma\varepsilon/P_s^2. \quad (3.14)$$

The length is material-dependent; the data in Table 1 give $l_0 = 1.5$ nm, using the 180° domain wall energy. Without this length or something else to replace it, the system lacks the dimensional information. For example, a system solely based on long range interactions—elastic, dielectric and piezoelectric—does not have any characteristic length scale. Neither does a system solely based on surface energy, such as growing grains, have a characteristic length scale. Note that, in identifying the length scale, we have used the ratio of the domain wall energy and dielectric energy. We can as well use the ratio $\Gamma/(\mu\gamma_s^2)$.

Normalizing all lengths by l_0 and equating the dimensions of the energy rate and dissipation rate in equation (3.6), we find a physical time scale

$$t_0 = \frac{l_0^2}{M\Gamma} = \frac{\Gamma\varepsilon^2}{MP_s^4}. \quad (3.15)$$

The data in Table 1 give $t_0 = 4.5 \times 10^{-13}$ s, using the 180° domain wall energy.

The relative magnitude of elastic and dielectric energy is measured by the dimensionless ratio

$$\frac{\mu\gamma_s^2}{P_s^2/\varepsilon}. \quad (3.16)$$

The relative magnitude of mechanical and electrical loads is measured by the dimensionless ratio

$$\frac{\sigma_\infty \gamma_s}{E_\infty P_s}. \quad (3.17)$$

The dimensionless ratio $\varepsilon E_\infty/P_s$ describes the magnitude of the applied electric field. The ratio is small because P_s/ε is much larger than the usual electric fields applied on ferroelectrics. For the crystal specified in Table 1, the applied field $E_\infty = 1.3$ MV/m corresponds to $\varepsilon E_\infty/P_s = 0.05$. One can similarly describe the level of mechanical loading with $\sigma_\infty/\mu\gamma_s$.

4. ONE DEGREE OF FREEDOM

Several simple situations are considered in this section. They can all be approximately described with one degree of freedom. The results are used to extract from experimental data parameters such as domain wall mobility and energy.

4.1. 180° domain spikes

When a single-domain crystal is placed into an electric field opposite to the polar direction, numerous 180° domain spikes emerge [13]. They grow much faster in the direction of the applied field than in the normal direction (Fig. 4). The sideways motion is not easily observed, unless under special conditions [20]. The forward velocity V was found experimentally to vary with the applied field E as [13]

$$V = M_0(E - E_0), \quad (4.1)$$

where M_0 and E_0 are the parameters to fit the experimental data ($M_0 = 2.5 \times 10^{-4}$ m²/V s and $E_0 = 0.22$ MV/m at the room temperature). The thickness of the spikes is of the order of $w = 1$ μm. In what follows, we interpret this experimental result in terms of our model.

A spike is taken to be a lamina, thickness w and length L, embedded in the parent crystal. The spike thickens at a much lower rate than it elongates. Consequently, we will assume that the thickness is constant, and that the spike has only one degree of freedom, its length L. The introduction of the spike

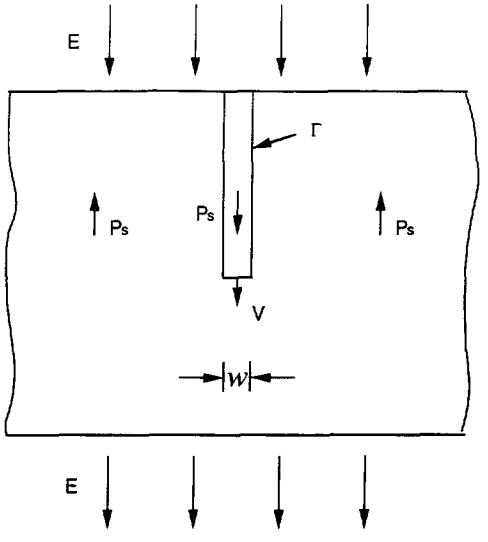

Fig. 4. Polarization reversal by a spike-like domain.

into the parent domain increases the free energy, per unit thickness of the crystal, by

$$G = -2P_sEwL + 2\Gamma L. \tag{4.2}$$

The first term is due to the external field in reversing the spontaneous polarization. The second term is due to the creation of the domain wall area. When $L \gg w$, the field around the spike tip is invariant as the spike elongates; it does not drive the spike motion and is excluded from equation (4.2). The piezoelectric effect is negligible.

The spike length, L, is the generalized coordinate. The force associated with the spike extending a unit distance is

$$f = -\partial G/\partial L = 2P_sEw - 2\Gamma. \tag{4.3}$$

The applied electric field drives the growth of the spike, and the domain wall energy resists it. The spike grows only if $f > 0$. Thus the minimum field needed to drive a spike is

$$E_0 = \frac{\Gamma}{P_s w}. \tag{4.4}$$

This relation affords an estimate of the domain wall energy. Taking the experimental values $w = 1\ \mu$m, $E_0 = 0.22$ MV/m and $P_s = 0.26$ C/m^2, we find that $\Gamma = 0.06$ J/m^2. This estimate is within the range estimated by other methods [21, 22].

Denote the generalized velocity by $\dot{L}$. The velocity normal to the domain wall is V projected to the normal direction. Since this one degree of freedom model cannot resolve the shape of the spike tip, we will take the tip to be flat—that is, every point on the domain wall at the tip has normal velocity V. Furthermore, the mobility is taken to be constant. The functional (3.6) becomes

$$\Pi(V) = -fV + \frac{V^2}{2M} w. \tag{4.5}$$

It minimizes when $\partial\Pi/\partial V = 0$, leading to

$$V = M(2P_sE - 2\Gamma/w). \tag{4.6}$$

A comparison with the experimental data of equation (4.1) gives an estimate of the domain wall mobility $M = M_0/2P_s = 4.8 \times 10^{-4}$ m^3/s N. We are unaware of any other independent estimate of the mobility.

4.2. 90° domain spikes

Figure 5 illustrates a single-domain crystal under a compressive stress along the polar axis and an electric field normal to the polar axis. Both tend to rotate the polar axis by 90°. It is observed experimentally that the spikes grow at 45° from the polar axis [23]. The free energy variation due to the introduction of the spike is [24]

$$G(L) = -(P_sE + \gamma_s\sigma)wL + 2\Gamma L. \tag{4.7}$$

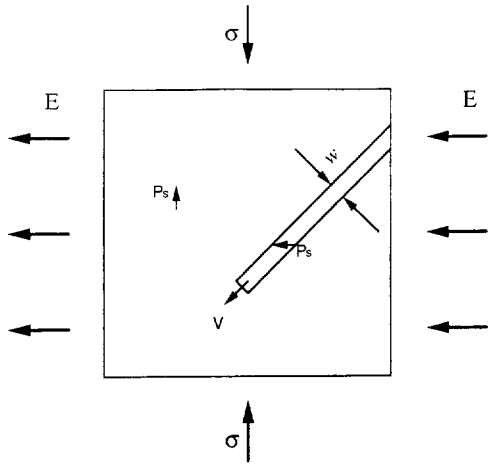

Fig. 5. Growth of a spike-like 90° domain.

The generalized force associated with the spike length is

$$f = -\partial G/\partial L = (P_sE + \gamma_s\sigma)w - 2\Gamma. \tag{4.8}$$

In the absence of electric field, equation (4.8) shows that the minimum stress needed to induce a spike is

$$\sigma_0 = \frac{2\Gamma}{w\gamma_s}. \tag{4.9}$$

Taking $w = 2\ \mu$m and the values of domain wall energy and the spontaneous strain in Table 1, we find this stress to be $\sigma_0 = 0.2$ MPa, which is close to the experimental value 0.22 MPa reported recently [25]. Conversely, the experimentally determined stress gives an estimate of the 90° domain wall energy.

4.3. Sideways motion

Figure 6 shows a thin crystal with a flat 180° wall, area A, propagating at a velocity V. The free energy is

$$G = -2P_sEAx \tag{4.10}$$

and the thermodynamic pressure on the domain wall is

$$p = -\frac{\partial G}{A\,\partial x} = 2P_sE. \tag{4.11}$$

This result is consistent with equation (2.10), taking $\kappa = 0$ and $D^- - D^+ = 2P_s$. According to the linear

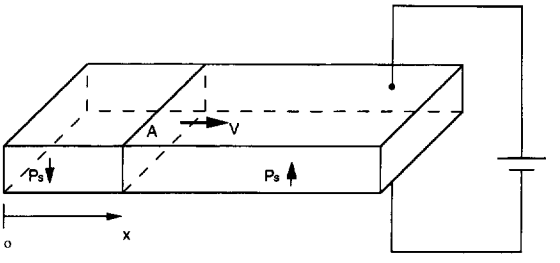

Fig. 6. Sideways motion of a domain wall in a thin crystal.

kinetic law, this pressure drives the domain wall to move at the velocity

$$V = 2MP_sE. \tag{4.12}$$

5. TWO DEGREES OF FREEDOM

Although the models of one degree of freedom provide useful relations, many questions remain unanswered. Why does a domain grow like a spike? What sets its width? We can answer these questions by evolving the nuclei with two degrees of freedom.

5.1. 180° domain nucleus

Figure 7 illustrates the cross-section of a cylindrical domain in a large parent domain having the opposite polarization. The energetics of this problem has been studied [26, 27]; we now apply the variational principle to study its kinetics. Because both domains have the identical spontaneous strain, the elastic and the piezoelectric effects are negligible compared to the dielectric effects. The problem is further simplified by assuming isotropic domain wall energy, permittivity and mobility. To avoid solving an electrostatic problem for complex-shaped inclusions, following Refs [26, 27], we approximate the cross-section of the domain by a sequence of ellipses, evolving the domain with two generalized coordinates, the semi-axes of α_1 and α_2.

Let (x_1, x_2) be the coordinate shown in Fig. 7. The ellipses are represented by

$$x_1 = \alpha_1 \cos\theta, \quad x_2 = \alpha_2 \sin\theta. \tag{5.1}$$

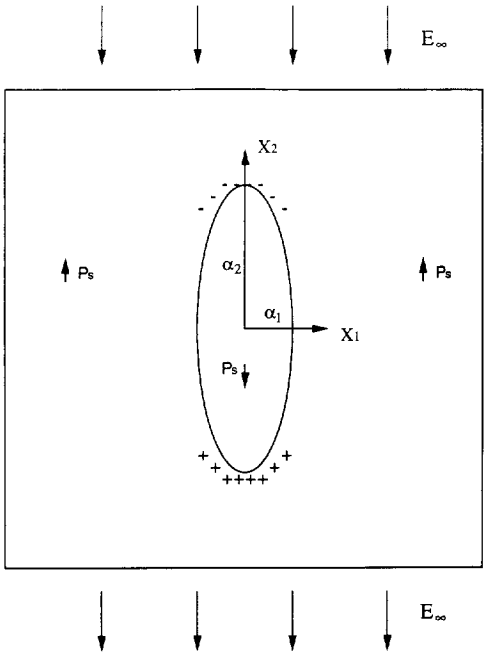

Fig. 7. A 180° domain nucleus.

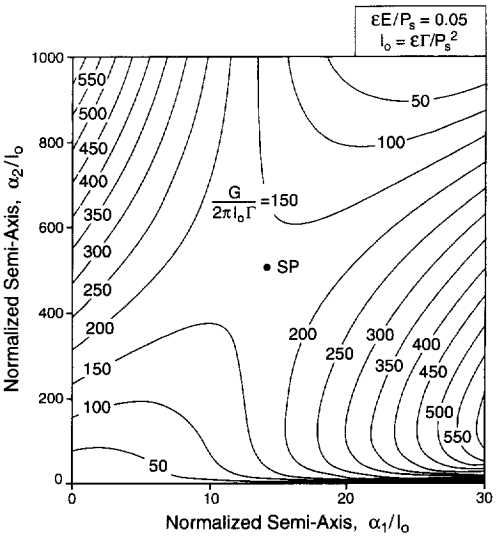

Fig. 8. Free energy contours for a 180° domain nucleus.

At a given time, the point (x_1, x_2) traces the entire ellipse as θ sweeps the interval $(0, 2\pi)$. The line element of the elliptic domain wall is

$$\mathrm{d}s = (\alpha_1^2 \sin^2\theta + \alpha_2^2 \cos^2\theta)^{1/2}\,\mathrm{d}\theta, \tag{5.2}$$

and the normal vector is

$$[n_1, n_2] = [\alpha_2 \cos\theta, \alpha_1 \sin\theta]\,\mathrm{d}\theta/\mathrm{d}s. \tag{5.3}$$

The virtual velocity of the domain wall is linear in the generalized velocities

$$\begin{aligned} U &= \dot{x}_1 n_1 + \dot{x}_2 n_2 \\ &= (\alpha_2 \cos^2\theta\,\mathrm{d}\theta/\mathrm{d}s)\dot{\alpha}_1 + (\alpha_1 \sin^2\theta\,\mathrm{d}\theta/\mathrm{d}s)\dot{\alpha}_2. \end{aligned} \tag{5.4}$$

The above relations completely specify the kinematics of the system.

The free energy due to the introduction of the nucleus into the parent crystal is [26]

$$G(\alpha_1, \alpha_2) = \Gamma s + \frac{2\pi\alpha_1^2\alpha_2 P_s^2}{\varepsilon(\alpha_1 + \alpha_2)} - 2P_sE_\infty\pi\alpha_1\alpha_2. \tag{5.5}$$

The first term is the domain wall energy, which resists the growth and tends to make the domain circular. The second term is the depolarization energy induced by the discontinuity of the spontaneous polarization, which strongly resists the growth in the α_1 direction, but only weakly resists the growth in the α_2 direction. The third term is the work term associated with polarization reversal, which drives the nucleus to grow and tends to make the nucleus circular.

Figure 8 shows the contours of constant levels of free energy, normalized as $G/(2\pi l_0\Gamma)$. The loading level for the simulation is $\varepsilon E_\infty/P_s = 0.05$. The free energy surface has a saddle point at around $\alpha_1 = 13l_0$ and $\alpha_2 = 500l_0$, indicated by SP in Fig. 8. The physical origin of this saddle point is evident. Along either the axis $\alpha_1 = 0$ or $\alpha_2 = 0$, when the needle-shaped domain elongates, both the work term and the depolarization

energy vanish, and the domain wall energy increases the total free energy. Along a path with a large aspect ratio α_2/α_1, the total free energy is low for both a very small and a very large nucleus, and reaches a peak for an intermediate one.

The fate of a nucleus depends on its initial position on the thermodynamic surface. To decrease the free energy, a very small nucleus shrinks, and a very large nucleus grows. For a nucleus near the saddle point, its fate is determined by both the energetics and the kinetics. In all cases, the free energy landscape alone does not determine the evolution path.

We next use the variational principle to calculate the evolution path and rate. The differential equations (3.12) become

$$\dot{\alpha}_1 = \frac{H_{22}f_1 - H_{12}f_2}{H_{11}H_{22} - H_{12}^2}, \quad \dot{\alpha}_2 = \frac{H_{11}f_2 - H_{12}f_1}{H_{11}H_{22} - H_{12}^2}. \tag{5.6}$$

The generalized forces and viscosities, in dimensionless form, are given by

$$f_1 = \frac{\varepsilon E_\infty}{P_s}\alpha_2 - \frac{\alpha_1\alpha_2(\alpha_1 + 2\alpha_2)}{(\alpha_1 + \alpha_2)^2} - \frac{2}{\pi}\int_0^{\pi/2} \frac{\alpha_1 \sin^2\theta \, d\theta}{(\alpha_1^2 \sin^2\theta + \alpha_2^2 \cos^2\theta)^{1/2}}$$

$$f_2 = \frac{\varepsilon E_\infty}{P_s}\alpha_1 - \frac{\alpha_1^3}{(\alpha_1 + \alpha_2)^2} - \frac{2}{\pi}\int_0^{\pi/2} \frac{\alpha_2 \cos^2\theta \, d\theta}{(\alpha_1^2 \sin^2\theta + \alpha_2^2 \cos^2\theta)^{1/2}}$$

$$H_{11} = \frac{2}{\pi}\int_0^{\pi/2} \frac{\alpha_2^2 \cos^4\theta \, d\theta}{(\alpha_1^2 \sin^2\theta + \alpha_2^2 \cos^2\theta)^{1/2}}$$

$$H_{22} = \frac{2}{\pi}\int_0^{\pi/2} \frac{\alpha_1^2 \sin^4\theta \, d\theta}{(\alpha_1^2 \sin^2\theta + \alpha_2^2 \cos^2\theta)^{1/2}}$$

$$H_{12} = H_{21} = \frac{2}{\pi}\int_0^{\pi/2} \frac{\alpha_1\alpha_2 \sin^2\theta \cos^2\theta \, d\theta}{(\alpha_1^2 \sin^2\theta + \alpha_2^2 \cos^2\theta)^{1/2}}.$$

Given initial semi-axes of a nucleus, we trace its evolution by numerically integrating equation (5.6). Figure 9 shows the evolution of a nucleus of initial axes $\alpha_2 = 550l_0$ and $\alpha_1 = 200l_0$. The α_2 axis increases almost linearly with the time after some initial adjustment. The α_1 axis decreases first, and then increases slowly relative to the α_2 axes. The behavior justifies the one degree of freedom approximation made in Section 4.1. We have also simulated the evolution of nuclei of other initial sizes, which are not included here for the sake of space.

5.2. *90° domain nucleus*

Figure 10 shows an elliptic 90° domain lying in the 45° from the stresses. The problem is analogous to mechanical twinning; see a recent contribution on the

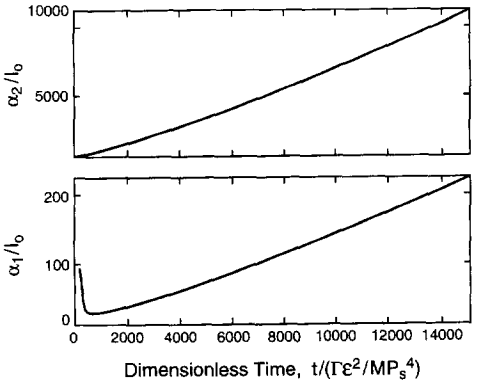

Fig. 9. The semi-axes of a 180° domain nucleus as functions of time.

subject [28]. The remote stress state is equivalent to a pure shear stress in the coordinate (x_1, x_2). The free energy due to the introduction of a domain nucleus is

$$G = \Gamma s + 2\pi\alpha_1\alpha_2(1 - 2S_{12})\mu\gamma_s^2 + \frac{\pi\alpha_1^2\alpha_2 P_s^2}{\varepsilon(\alpha_1 + \alpha_2)} - (E_\infty P_s + 2\sigma_\infty\gamma_s)(\pi\alpha_1\alpha_2), \tag{5.7}$$

with

$$S_{12} = \frac{1}{4(1-\nu)}\left[\frac{\alpha_1^2 + \alpha_2^2}{(\alpha_1 + \alpha_2)^2} + 1 - 2\nu\right],$$

and ν being Poisson's ratio. The first term in equation (5.7) is the domain wall energy, the second the residual strain energy [29], the third the depolarization energy, and the last the work done by the remote loads in switching. The qualitative behaviors are similar to the 180° nucleus and will not be repeated here. In deriving equation (5.7), we have ignored the piezoelectric effect; a complete treatment should invoke the piezoelectric inclusion solution [30].

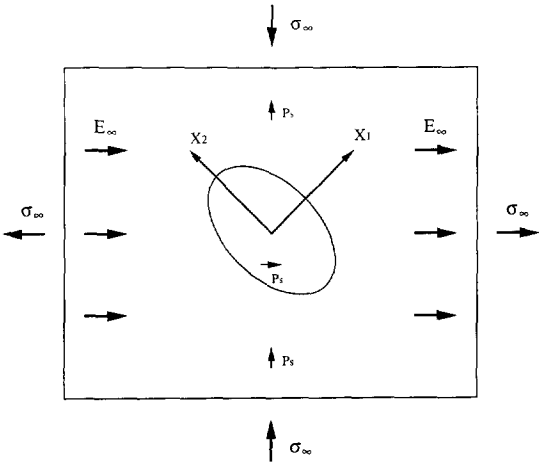

Fig. 10. A 90° domain nucleus.

6. CONCLUDING REMARKS

In this paper, we present a variational principle for ferroelectric domain evolution. One may choose to model an evolving domain structure with any kind and any number of generalized coordinates, depending on prior knowledge and the level of details to be resolved. We illustrate this approach with examples where one or two degrees of freedom can capture the major features. The general approach fits naturally into the framework of finite element method, and will be a robust simulation tool.

The variational principle has been used in modeling several evolution problems, including diffusion [31], creep voids [32], powder sintering [33, 34]. However, its general applicability has not been appreciated, particularly in problems with complex energetics and structural changes. Following Gibbs [35], we picture the free energy function as a surface in the space spanned by the free energy and the generalized coordinates. A point on the surface represents a state of the crystal, and the slopes of a tangent plane contacting the point represent the generalized forces. The variational principle adds another property to every point on the thermodynamic surface: a viscosity matrix. We have used the idea to model other energetic-kinetic problems, including grain growth [36], void shape instability [37, 38], dislocation climb [39], wrinkling of oxide scales on high temperature alloys [40] and electromigration transgranular slits [41]. It is hoped that a general-purpose finite element program will soon succeed in simulating diverse phenomena of structural evolution in materials.

Acknowledgements—The work was supported by the Belgian–American Educational Foundation (RL), by the Office of Naval Research through contract N00014-93-1-0110, and by the National Science Foundation through a Young Investigator Award MSS-9258115 (ZS).

REFERENCES

1. R. Landauer, D. R. Young and M. E. Drougard, *J. appl. Phys.* **27,** 752 (1956).
2. R. C. Miller and A. Savage, *Phys. Rev.* **115,** 1176 (1959).
3. B. Jaffe, W. R. Cook and H. Jaffe, *Piezoelectric Ceramics*. Academic Press, New York (1971).
4. K. A. Esaklul, W. W. Gerberich and B. G. Koepke, *J. Am. Ceram. Soc.* **63,** 25 (1980).
5. Q. Jiang, W. Cao and L. E. Cross, *J. Am. Ceram. Soc.* **77,** 211 (1994).
6. J. E. Burke and D. Turnbull, *Prog. Metal Phys.* **3,** 220 (1952).
7. H. J. Frost, C. V. Thompason and D. T. Walton, *Acta metall. mater.* **38,** 1455 (1990).
8. Q. Jiang, *J. Elasticity* **34,** 1 (1994).
9. R. Abeyaratne and J. K. Knowles, *J. Mech. Phys. Solids* **38,** 345 (1990).
10. I. Prigogine, *Introduction to Thermodynamics of Irreversible Processes*, 3rd. ed. Wiley, New York (1967).
11. F. Jona and G. Shirane, *Ferroelectric Crystals*. Pergamon Press, Oxford (1962).
12. A. F. Devonshire, *Phil. Mag.* **3,** 85 (1954).
13. W. J. Mertz, *Phys. Rev.* **95,** 690 (1954).
14. R. C. Miller and G. Weinreich, *Phys. Rev.* **117,** 1460 (1960).
15. J. D. Eshelby, in *Solid State Physics*, Vol. 3, pp. 79–144 (1956). Academic Press, New York.
16. S. Socrate and D. M. Parks, *Acta metall. mater.* **41,** 2185 (1993).
17. C. Herring, in *Physics of Powder Metallurgy* (edited by W. E. Kingston). McGraw-Hill, New York (1951).
18. W. W. Mullins, *J. appl. Phys.* **28,** 333 (1957).
19. R. J. Asaro and W. A. Tiller, *Metall. Trans.* **3,** 1789 (1972).
20. R. C. Miller and A. Savage, *Phys. Rev.* **112,** 755 (1958).
21. W. Kinase and H. Takahasi, *J. Phys. Soc. Japan* **12,** 464 (1957).
22. V. A. Zhirnov, *Soviet Physics JETP* **35,** 822 (1959).
23. E. A. Little, *Phys. Rev.* **98,** 978 (1955).
24. Z. Suo, in *Smart Structures and Materials* (edited by A. V. Srinivasan), pp. 1–6. American Society of Mechanical Engineers, New York (1991).
25. Z. Li, C. M. Foster, X.-H. Dai, X.-Z. Xu, S.-K. Chan and D. J. Lam, *J. appl. Phys.* **71,** 4481 (1992).
26. R. Landauer, *J. appl. Phys.* **28,** 227 (1957).
27. P. Rosakis and Q. Jiang, *Int. J. Engng Sci.* **33,** 1 (1995).
28. P. Rosakis and H. Tsai, *Int. J. Solids Structures* **32,** 2711 (1995).
29. J. D. Eshelby, *Proc. R. Soc.* **A241,** 376 (1957).
30. H. Sosa, *Int. J. Solids Structures* **28,** 491 (1991).
31. M. A. Biot, *Variational Principles in Heat Transfer*. Oxford University Press, Oxford (1970).
32. A. Needleman and J. R. Rice, *Acta metall.* **28,** 1315 (1980).
33. R. M. McMeeking and L. T. Kuhn, *Acta metall.* **40,** 961 (1992).
34. A. C. F. Cocks, *Acta metall.* **42,** 2197 (1994).
35. J. W. Gibbs, *The Scientific Papers, Vol. I, Thermodynamics*. Ox Bow Press, Connecticut (1993).
36. Z. Suo, in *Advances of Applied Mechanics* (edited by J. W. Hutchinson and T. Y. Wu), Vol. 33, in press.
37. Z. Suo and W. Wang, *J. appl. Phys.* **76,** 3410 (1994).
38. B. Sun, Z. Suo and A. G. Evans, *J. Mech. Phys. Solids* **42,** 1653 (1994).
39. Z. Suo, *Acta metall. mater.* **42,** 3581 (1994).
40. Z. Suo, *J. Mech. Phys. Solids* **43,** 829 (1995).
41. W. Q. Wang, Z. Suo and T. H. Hao, *J. appl. Phys.* In press (1996).